



Cognitive radio resource scheduling using an adaptive multiobjective evolutionary algorithm

Hongbo Wang^{1,2} · Yizhe Wang^{1,2} · Fanbing Zeng¹ · Jin Wang¹

Accepted: 11 March 2024 / Published online: 19 March 2024
© The Author(s) 2024

Abstract

With the proliferation of IoT devices and the increasing popularity of location-oriented services in cyber-physical-social systems, the cognitive engines of these systems have taken on a multitude of parameters across various dimensions, making it impractical and time-consuming to search for the exact optimal solution. To address this challenge, the use of nature-inspired or evolutionary algorithms to find satisfactory solutions in a timely manner has gained significant attention, with reference point-based algorithms being one of the prominent approaches. However, when dealing with nonuniform, degenerate, and discrete Pareto fronts in the target space, using a considerable number of reference points may become ineffective, leading to a loss of diversity in exploration and exploitation during the problem-solving process. Consequently, the distribution of the solutions is adversely affected. To overcome this challenge, this paper presents a strategy to estimate the eigenvalues of the Pareto front in a timely manner. When encountering nonuniform, degenerate, and discrete Pareto fronts, a combination of radial space partitioning and angle selection mechanisms is employed to address these issues. Subsequently, an adaptive selection-based many-objective evolutionary algorithm (ASMaOEA) is proposed. Extensive comparisons with several competing methods on 31 representative benchmark problems demonstrate that ASMaOEA can provide a flexible configuration for decision engines in three typical scenarios involving cyber-physical-social systems. Furthermore, the analysis confirms that ASMaOEA can reduce the bit error rate and improve the system's throughput, thereby offering substantial benefits to the overall performance of the system.

Keywords Cognitive engine · Resource scheduling · Adaptive selection · Multiobjective optimization

1 Introduction

With rapid advances in wireless client and sensor-oriented applications, especially with the arrival of the 5G era, the available spectrum of resources faces pressure towards increased distribution, as the IPv4 address protocol of the

Internet did 20 years ago. However, measurements of the radio spectrum indicate that the rate of utilization of currently allocated frequency bands is very low [1]. It is useful to analyse the reasons for this phenomenon. Suppose a spectrum resource has two frequencies, namely, a licenced band and an unlicensed band. If they are allocated to users in static form [2], this helps resolve the disorder in utilization to a certain extent, but it also leads to the selfish use of an exclusive mode. That is, authorized users do not allow unauthorized users to see any information, even during idle periods, and this does not suit the demand for dynamic access without intervention. In this context, the concept of the cognitive radio was developed. The basic purpose of the cognitive engine (CE) is to adjust its operating parameters according to the conditions of the available channels and user requirements and provide a flexible configuration, and this has been a subject of interest for researchers. CR technology is a spectrum allocation technology capable of self-analysis and decision-making. Its most prominent feature is that it can automatically analyse

Yizhe Wang, Fanbing Zeng, and Jin Wang contributed equally to this work

✉ Hongbo Wang
foreverwhb@126.com

Yizhe Wang
wangyz_09@163.com

¹ School of Computer and Communication Engineering, University of Science and Technology Beijing, Beijing 100083, China

² Beijing Key Laboratory of Knowledge Engineering for Materials Science, University of Science and Technology Beijing, Beijing 100083, China

the radio spectrum environment within the system to determine the idle spectrum. If the primary user does not disturb the transmission of information, the secondary user can reuse it, which can improve the spectrum efficiency.

Cognitive radio scheduling is an NP-hard problem. The spectrum allocation strategy and optimization algorithm strongly affect the performance of cognitive radio systems. Spectrum utilization, energy consumption and cost efficiency are three key performance indicators that should be studied together when developing sustainable 5G systems [3]. Considering that spectrum allocation often needs to account for multiple conflicting objectives at the same time, the spectrum allocation scheme for a single objective cannot meet the actual needs, so the optimization of spectrum allocation can be regarded as a multiobjective optimization problem based on spectrum efficiency, energy consumption and cost efficiency.

The reference point-based approach enables decision-makers to define a set of reference points based on their priorities and preferences. By providing a range of solutions that are close to these reference points, this approach offers a greater variety of choices and enhanced decision support. This empowers decision makers to select the best solution from the nondominated solution set, which better aligns with their objectives. However, the diversity of solutions in reference point-based multiobjective optimization algorithms heavily relies on the selection mechanism of reference points. In optimization problems with nonuniform, degenerate, or discontinuous Pareto fronts, using numerous reference points can become ineffective, resulting in a lack of solutions. Conversely, using a small number of reference points may yield many solutions, significantly impacting the diversity of the Pareto solution set.

To address the limitations of the algorithm in handling degenerate, discontinuous, and nonuniform optimization problems, our proposed method is a flexible adaptive selection mechanism based on the many-objective evolutionary algorithm (ASMaOEA) that incorporates radial space partitioning, adaptive Pareto front detection, and angle selection mechanisms to further enhance performance. By utilizing radial space partitioning, the solution space is divided into regions based on the reference points. This approach ensures a more balanced distribution of the solutions and helps mitigate the issue of clusters near a few reference points. Additionally, the adaptive Pareto front detection technique dynamically identifies the regions of interest in the solution space. This adaptability allows for efficient exploration and exploitation of the Pareto front, even in scenarios where the front is degenerate or discontinuous.

This paper is based on a reference point-based multiobjective evolutionary algorithm θ -DEA [4], which defines a set of reference points that are evenly distributed in the target space with clustering and adopts the novel θ -dominant mechanism.

We propose a new algorithm, ASMaOEA, by improving the selection mechanism and environment strategy of θ -DEA's predecessor. In the experiments, ASMaOEA achieved good convergence and diversity in the test problems and cognitive radio applications.

The remainder of this article is structured as follows. Section 2 provides a brief description of related work that is commonly considered the state of the art. In Section 3, the features of the system model and problem formulation are analysed in detail. Section 4 presents a flexible adaptive selection mechanism based on the many-objective evolutionary algorithm (ASMaOEA) according to the real-time requirements of the cognitive radio resource schedule. In Sections 5 and 6, we focus on the experimental analysis and comparison, respectively, based on benchmark functions and the first type of problem of cognitive radio (CRF1). Section 7 provides the conclusions of this paper, with a discussion of our ongoing and future work.

2 Related work

Some typical related research, including case-based reasoning (CBR), has been used to design CEs in IEEE 802.22 networks [5]. A CR engine platform for developing available frequency channels in tactical wireless sensor networks uses case-based reasoning to locate available channels to achieve high-fidelity dynamic spectrum access (DSA) [6]. The reasoning engine and knowledge base are the keys to realizing CBR. A comprehensive knowledge base can often achieve better matching and decision-making. In contrast, when the scenarios encountered cannot be matched in the knowledge base, the method will become inefficient.

In recent years, artificial neural networks have shown strong adaptability. A learning engine framework based on the support vector machine (SVM) has been used to configure radio parameters, and its bit error rate (BER) and signal-to-noise ratio (SNR) have been estimated [7]. Eisen et al. proposed a variant of a graph neural network, the random edge graph neural network (REGNN), which takes the channel and node states as inputs and combines them through a nonlinear graph convolution filter to obtain the resource allocation function [8]. In [9], the optimization objective was defined as the loss function, and to minimize this objective, the model aimed to find the most favourable output. However, since the neural network involves many parameters, when the network is large, it may take a long time to prepare, and the accuracy of the model is strongly dependent on the training data.

Several researchers have applied the genetic algorithm (GA), a simple random heuristic query strategy, to the design of cognitive engines. Rondeau et al. applied the GA to determine the parameters of a software-defined radio (SDR) to

meet the user's QoS requirements [10]. An adaptive GA-based cognitive engine was proposed in [11] to tune radio parameters. Furthermore, many hybrid cognitive engines have been introduced. They aim to combine learning and optimization algorithms to perform more efficient system adaptation. Heuristic techniques are widely employed for decision making in CEs. Researchers have exploited the advantages of the quantum GA to design a hybrid engine with CBR [12]. Ashwin et al. proposed a hybrid engine based on CBR and the GA that has the capability to adapt to new environments using the GA [13]. GAs handle multiobjective enhancement issues, consume less memory and are faster when examining vast regions. However, the design of a GA depends on the specific problems to be solved, and determining the chromosome representation of parameters, domains and ranges is challenging. In addition, the slow convergence speed and poor local search ability of the GA are problematic.

Other intelligent optimization algorithms, for example, ant colony optimization (ACO), have been proposed for CE design [14–16]. Another hybrid approach was investigated in [17], where CBR and particle swarm optimization (PSO) were used as the core of CE. To reduce the complexity of the formula for accurate outage probability, PSO was used in [18] to determine the best secondary user (SU) transmission power. Yadav et al. proposed their own federated cloud computing framework based on matching and multiround allocation (MMA) [19], which included hybrid chaotic particle search (HCPS), a modified artificial bee colony (MABC), and modified cuckoo search (MCS) [20].

Among the many intelligent optimization algorithms, multiobjective evolutionary algorithms perform well. Liu et al. proposed a resource allocation paradigm for spectrum allocation in cognitive radio based on graph theory. Based on the proposed objective problem and model, the ant colony optimization algorithm was improved by introducing the differential evolution (DE) process and designing variable-neighbourhood-search DE. Through the simulation data verification, the improved technical performance was shown to be better [21]. In 2020, the evolutionary computation method was thoroughly examined in research on the energy harvesting (EH) method in the multi-input single-output CRN (MISO CRN) [22]. Abbasi et al. presented an optimized cascade chaotic fuzzy system (OCCFS) [23]. OCCFS incorporates fuzzy reasoning, neural network self-adaptation, chaotic signal generation, and cascade system generalizability in a unique structure optimized using the DE algorithm, and it outperformed other methods in terms of accuracy and efficiency.

Further improvement research on reference point-based optimization algorithms, represented by NSGA-III [24], has also gained significant attention from researchers. The NSGA-III emphasizes diversity when dealing with high-

dimensional multiobjective optimization problems but still lacks convergence pressure. Yuan et al. introduced a novel dominance mechanism, θ -DEA, to simultaneously ensure the convergence and diversity of the algorithm [4].

It is helpful to calculate individual density in the case of nondomination, and better individuals increase their density with other individuals, excluding poor individuals from diversity strategies [25]. In a two-stage strategy, in the first stage, the target number is not only considered for the constraint, and the second phase optimizes the objective function and the constraint at the same time [26]. A reference vector guides the EA for multiobjective optimization, decomposes the original multiobjective optimization problem into multiple single-object subproblems, and selects a preferred subset of the entire Pareto boundary according to user preference [27]. A custom-made evolutionary algorithm was proposed based on decision variable clustering [28]. A reference direction with a density estimator provided some new fitness allocations for schemes and environment selection strategies, which was helpful for improving the performance of the evolutionary algorithm [29].

With the increase in the number of optimization targets, selection pressure based on the Pareto dominance multiobjective optimization algorithm leads to slow convergence and poor optimization effects. Li et al. proposed AdaW based on MOEA/D, which regularly updates the weights by comparing the current evolutionary population with a well-maintained archive set to optimize the solution set [30].

3 System model

The CE involves many parameters that need to be adjusted to improve the system's performance. Generally, the overall requirements of objectives such as the bit error rate, transmission power, and throughput should be considered when allocating related spectrum resources. Assume that the parameter vector is $X = \{x_1, x_2, x_3, \dots, x_n\}$ and that the objective function is $F = \{f_1, f_2, f_3, \dots, f_{m_t}\}$, where n is the number of decision variables and m_t is the number of target functions. These variables include the transmission power, modulation scheme, modulation order, coding rate, time division duplex, and sampling rate, and the related targets include the minimization of the BER and power and the maximization of the throughput.

The ideal optimal values of the above multiple objective functions are difficult to satisfy at the same moment. For example, reducing the bit error rate usually means that the transmit power must increase. We hope to obtain some trade-off solutions for each objective function without knowing any preferences; that is, we aim to obtain the Pareto front of the related problem. To understand the system model, we start

from the first type of problem of cognitive radio (abbreviated CRF1), where two decision variables are included (signal power P and modulation order M), and this model meets the conditions of the modulation index $m = \log_2 M$.

3.1 Problem formulation of CRF1

3.1.1 Minimize the bit error rate function f_{be}

The bit error rate P_{ei} is an important performance indicator in all communication systems. The channel type, modulation method, and signal-to-noise ratio all affect its value. Notably, different modulation methods have different calculation formulae for P_{ei} . The details are as follows.

In the AWGN channel environment, for an MPSK modulation, the bit error rate P_{ei} can be expressed as in (1):

$$P_{ei} = \frac{2}{\log_2 M} Q\left(\sqrt{2\log_2 M \cdot \gamma} \cdot \sin \frac{\pi}{M}\right) \quad (1)$$

For MQAM modulation, the bit error rate P_{ei} is expressed by (2).

$$P_{ei} = \frac{4}{\log_2 M} \left(1 - \frac{1}{\sqrt{M}}\right) Q\left(\sqrt{\frac{3\log_2 M}{M-1} \cdot \gamma}\right) \quad (2)$$

In (1) and (2), M is the modulation order, $Q(\cdot)$ is a Gaussian function, and its expression is shown in (3).

$$Q(z) = \frac{1}{\sqrt{2\pi}} \int_z^{\infty} \exp\left(-\frac{x^2}{2}\right) dx \quad (3)$$

where γ is the bit-to-noise ratio (BNR) of the receiver signal, which is the ratio of the power to the noise of each bit signal E_b/N_0 . E_b is related to the received signal power S , the symbol rate R_s and the modulation system M . The related functions can be written as (4) and (5).

$$E_b = \frac{S}{R_s \log_2 M} \quad (4)$$

$$S = P_w - P_l \quad (5)$$

In (5), P_w is the transmission power, and P_l is the path loss. Since the total signal noise energy N equals the product of N_0 and the bandwidth B , γ can be expressed by (6).

$$\begin{aligned} \gamma &= \frac{E_b}{N_0} = 10 \log_{10} \left(\frac{S}{R_s \cdot N_0 \cdot \log_2 M} \right) \\ &= 10 \log_{10} \left(\frac{B}{R_s \cdot \log_2 M} \right) \end{aligned} \quad (6)$$

Assuming that the maximum allowable bit error rate is 0.5, the objective function for minimizing the normalized bit error rate can be represented by (7). Here, S_n denotes the number of subcarriers, and P_{ei} represents the bit error rate of the i -th subcarrier.

$$f_{be} = \frac{\log_{10} 0.5}{\frac{1}{S_n} \cdot \sum_{i=1}^{S_n} \log_{10} P_{ei}} \quad (7)$$

3.1.2 Minimizing the energy consumption function f_p

There are numerous factors that influence the energy efficiency of a system, including the transmit power, channel bandwidth, modulation scheme, symbol rate, and other parameters that are involved in the complexity of system design. Considering the parameters of the channel bandwidth, modulation scheme, and symbol rate as the main factors, the transmission power of the signal can be expressed by (8).

$$\begin{aligned} f_p &= \rho_1 \times \frac{\sum_{i=1}^{S_n} P_{wi}}{S_n \times P_{\max}} + \rho_2 \times \frac{\sum_{i=1}^{S_n} P_{si}}{S_n \times P_s^{\max}} \\ &\quad + \rho_3 \times \frac{\sum_{i=1}^{S_n} \log_2 M_i}{S_n \times \log_2 M_{\max}} \end{aligned} \quad (8)$$

where ρ_1 , ρ_2 and ρ_3 represent the weight factors of the transmit power, modulation index and symbol rate, respectively. P_{\max} , P_s^{\max} , and M_{\max} denote the maximum values of transmit power, symbol rate, and modulation order allowed by the system, respectively. P_{wi} , P_{si} , and M_i represent the transmit power, symbol rate, and modulation order of the i -th subcarrier, respectively.

3.1.3 Maximizing the data rate function f_{thr} .

Some real-time applications require the support of high-speed data transmission, such as multimedia services and video meetings. Throughput can be used as an effective indicator of capacity, which indicates the amount of data that can be transmitted in one second. The calculation of throughput needs to consider many factors, such as the packet error rate, coding correction, and retransmission. This paper mainly aims at optimizing the parameters of the physical layer and does not consider the retransmission mechanism of the link layer. The bit rate of the transmitted data can be expressed as in (9), where R_c is the coding rate.

$$\text{Data_rate} = R_s \cdot \log_2 M \cdot R_c \quad (9)$$

In multicarrier systems, the normalized maximum data rate (throughput) function is given by (10).

$$f_{thr.} = 1 - \frac{\frac{1}{S_n} \left(\sum_{i=1}^{S_n} \log_2 M_i \cdot R_{si} \cdot R_{ci} \right) - \log_2 M_{\min} \cdot R_s^{\min} \cdot R_c^{\min}}{\log_2 M_{\max} \cdot R_s^{\max} \cdot R_c^{\max} - \log_2 M_{\min} \cdot R_s^{\min} \cdot R_c^{\min}} \quad (10)$$

where R_{ci} is the coding rate assigned to the i -th subcarrier. R_c^{\max} , R_c^{\min} , and R_s^{\max} are the maximum coding rate, minimum coding rate, and minimum symbol rate allowed by the system, respectively.

3.2 Dependencies among the three objective functions

Table 1 summarizes the parameters corresponding to the objective functions f_{be} , f_p and $f_{thr.}$. There is a complex dependence relationship between each objective function and its main parameters.

In Fig. 1, if a line with a solid black arrow points from a function node A to a parameter node B, A has a direct correlation with B. For example, f_{be} points to the three nodes P_w , R_s and M , which indicates that the value f_{be} will change according to these three parameters. Some parameters have a simultaneous influence on multiple objective functions, creating indirect constraint relationships between the objective functions, as illustrated by the red dashed lines in Fig. 1. This makes it impossible to achieve optimal values for all the objectives simultaneously. Trading off among these multiple interacting objective functions to suit the requirements of the user’s application and time-varying communication environment is the key task of the CE.

3.3 Coding mechanism of the decision domain

During cognitive radio parameter optimization, the coding mechanism of the decision domain describes an important task. The modulation order is discrete, so the two decision variables can encode a binary term. The transmit power varies from 0 to 25.2 dBm. Normally, the interfrequency band between them is 0.4 dBm, where a total of 64 values are obtained using 6 binary codes c_1, c_2, \dots, c_6 . Moreover, the

Table 1 The objective functions and their parameters

Objective function	Corresponding parameter
f_{be}	P_w, P_t, M, B, R_s, S_n
f_p	P_w, R_s, M
$f_{thr.}$	R_s, M, R_c

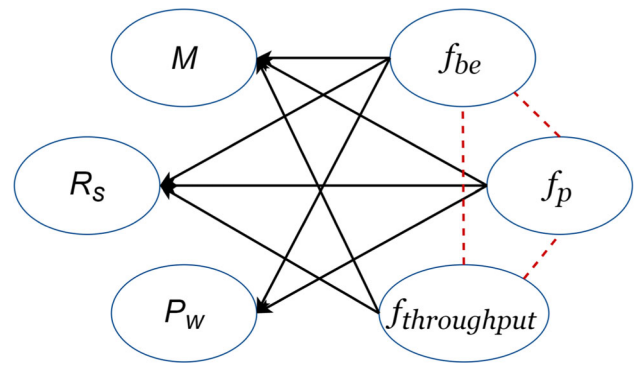


Fig. 1 Correlations among multiple objectives and parameters

modulation includes four patterns, namely, BPSK, QPSK, 16QAM and 64QAM. For $M = \{2, 4, 16, 64\}$, with two binary representations of c_7 and c_8 , single-subcarrier encoding requires one byte. For example, a subcarrier that has a transmit power of 2.8 dBm and a modulation scheme of 16QAM is coded as 11100011. Assuming that the number of subcarriers is L , the length of a single individual is $c_i * L$; therefore, when there are 32 subcarriers, a single individual adopts 256 bits of encoding [31, 32].

4 Improvement of the cognitive engine

In the reference point-based evolutionary algorithm, the aggregation operation may attract individuals to a reference point (or the neighbourhood of a reference point), such as in NSGA-III [24] and θ -DEA [4]. When a degenerate or discrete Pareto front is encountered, some reference points may not be able to obtain the final solution to the relevant problem in the cognitive decision space. A suitable method for scientifically measuring the occurrence of nonuniform, degenerate, and discrete conditions in the current optimization problem needs to be identified.

4.1 Adaptive detection of the pareto front

Assume that the given generation is t , and the given population obtains the number of niches τ_j (niche count), where $j = 1, \dots, N$ for each reference point after the clustering stage. By default, the number of reference points and the number of groups are the same; when $\tau_j > 0$, the j -th reference point is valid in the t -th generation. Let E_j represent the effective number of times during the period from the 0-th to t -th iterative calculation, and let the confidence degree be denoted as $p_e \in (0, 1)$. If $E_j^t \geq p_e \times t$ is satisfied, the j -th reference point is valid, and the operation statement $R_e^t = R_e^t + 1$ is carried out. Namely, the number of effective reference points in the current group can be

calculated according to the following (11):

$$R_e^t = \sum_{j=1, E_j^t \geq p_e * t}^N 1 \quad (11)$$

With the set $R_e = \{R_e^1, R_e^2, \dots, R_e^i, \dots, R_e^T\}$, T is the maximum iteration of the population evolution. If the following condition in (12) is satisfied, a Pareto front with a discrete or degenerate nonuniform situation will occur with a high probability.

$$\sqrt{\sum_{j=i}^{i+K-1} (R_e^j - \frac{1}{K} \sum_{t=i}^{i+K-1} R_e^t)^2} < \epsilon, i = 1, \dots, N - K \quad (12)$$

Here, ϵ is the fluctuation threshold for the number of reference points and is set to 3 according to the recommendation. K is an interval constant, and generally, $K \in [15, 50]$. We select the typical test function DTLZ2 to analyse the best value of k . For the 3-objective DTLZ2 function, the group size N is 210, with k values of 15, 20, 25, 30, 35, 40, 45 and 50, and five independent experiments are carried out according to different k parameters. Except for the parameters being tested, the other parameters are set to their defaults. We perform parameter sensitivity analysis using the inverted generational distance (IGD) metric. For detailed information about IGD, please refer to Section 5.1.1. Figure 2 shows the IGD mean and average running time of DTLZ2 for different k values. When K is 15, the average IGD index reaches the optimal value, and the average running time is close to the optimal value. After comprehensive consideration, we take K as 15 for the remaining investigations. ϵ denotes the fluctuation threshold of the reference point, and after a similar

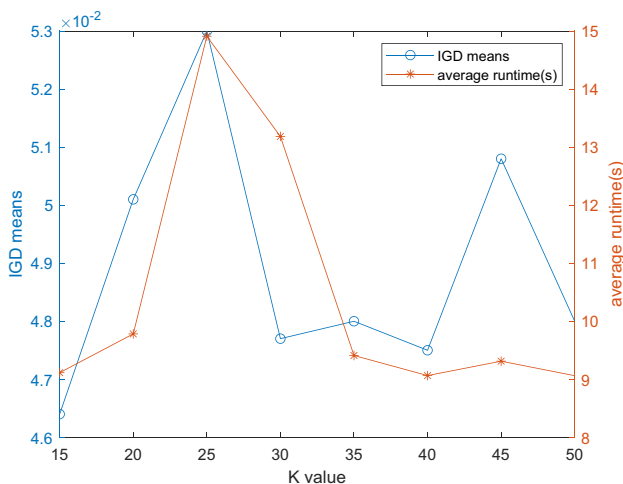


Fig. 2 The IGD mean and average running time of DTLZ2 with different k values

verification process, we conclude that its default value should be 3 for the CRF1 problem.

4.2 Adaptive selection flow and pseudocode

With the above decisive conditions of the Pareto front features, we can adaptively select the appropriate operation for a degraded and discrete frontier; this is called the adaptive selection-based many objective evolutionary algorithm (ASMaOEA). The ASMaOEA algorithm consists of three important steps: 1) determining the initial relevant parameters, such as population size, crossover and mutation factors, for generating the next individuals; 2) switching during nondominated sorting between two adaptive strategies (θ cluster or angle environment) according to the condition of the Pareto front features; and 3) using the whole group to construct the next generation. The algorithm loops these operations until its termination conditions are met. The detailed process is shown in Algorithm 1.

Algorithm 1 The pseudocode of ASMaOEA.

Require: N : size of the group; p_c : crossover probability; η_c : distribution index; T : maximum number of iterations

Ensure: A set of effective solutions for the given problems

```

1: Set the current iteration  $t = 0$ .
2: Set the random solution  $P_0 = \{X_1^0, X_2^0, \dots, X_N^0\}$ , a reference point set  $\wedge$ , and the ideal points  $\mathbf{z}^*$  and  $\mathbf{z}^{nad}$ , where  $\mathbf{z}^*$  and  $\mathbf{z}^{nad}$  are  $m$ -dimensional vectors formed by the minimum and maximum values of the current population  $P_0$  in each objective function.
3: while  $t \leq T$  do
4:    $S_t = \emptyset, P_{t+1} = \emptyset, i = 1, Q_t = \emptyset$ 
5:    $H = \text{RGDMatingSelection}(P_t, \mathbf{z}^*, \mathbf{z}^{nad})$  // Generate the mating pool  $H$  based on the spatial partition
6:    $Q_t = \text{SBXCrossover} + \text{NonUniformMutation}(P_t, H)$ 
7:    $(F_1, F_2, \dots) = \text{Nondominated-sort}(Q_t \cup P_t)$ 
8:   while  $|S_t| < N$  do
9:      $S_t = S_t \cup F_i$ 
10:     $i = i + 1$ 
11:  end while
12:  UpdateIdealAndNadirPoint( $F_1, \mathbf{z}^*, \mathbf{z}^{nad}$ )
13:  if  $t > T * \alpha$  and is ParetoNonUniform then
14:     $P_{t+1, N_0} = \theta$ -dominated-selection( $S_t, \mathbf{z}^*, \mathbf{z}^{nad}, \wedge, N_0$ ) // Select  $N_0$  individuals from  $S_t$  using nondominated sorting-based environmental selection
15:     $P_{t+1, N_1} = \text{angle-based-selection}(S_t / P_{t+1, N_0}, N_1, U)$ 
16:     $P_{t+1} = P_{t+1, N_0} \cup P_{t+1, N_1}$  // Select  $N_1$  others from  $S_t$  using angle-based environmental selection
17:     $t = t + 1$ 
18:  else
19:     $P_{t+1} = \theta$ -dominated-selection( $S_t, \mathbf{z}^*, \mathbf{z}^{nad}, N$ ) // Select  $N$  individuals from  $S_t$  using nondominated sorting-based environmental selection
20:     $R_e^t = \text{usableReferenceCount}(P_{t+1}, \mathbf{z}^*, \mathbf{z}^{nad})$  // Calculate the number of effective reference points in the current population
21:     $R_e = R_e \cup R_e^t$ 
22:     $t = t + 1$ 
23:  end if
24: end while

```

For better understanding, there are a few important points about the above Algorithm 1.

1) Let the reference set be denoted as $\wedge = \{\lambda_1, \lambda_2, \dots, \lambda_N\}$, where $\lambda_j = (\lambda_{j,1}, \lambda_{j,2}, \dots, \lambda_{j,m_t})^T$ and $j \in \{1, 2, \dots, N\}$, m_t is the number of objective functions.

2) The mating pool H in line 5 is based on space division, and it is used to select individuals in P_t as parents for crossing and mutation. After obtaining N offspring individuals Q_t and carrying out nondominated sorting of $Q_t \cup F_t$, we obtain $F_1, F_2, \dots, S_t = \cup F_i (i = 1, 2, \dots, L)$, where L is the minimum value for $|S_t|$.

3) Line 12 uses F_1 to update the ideal points Z^* and Z^{nad} . We judge the current iteration $t > T * \alpha$, where $\alpha \in [0, 1]$ in line 13. If this holds true, we need to further determine whether the Pareto front is nonuniform according to (12) in Section 4.1. When both conditions are satisfied at the same time, we need to select N_0 individuals (effective reference points) from S_t based on the nondominated sorting

environment and select N_1 others from S_t based on the angle method while keeping $N = N_0 + N_1$ true.

4.3 Sensitivity analysis of parameters

This subsection describes a sensitivity analysis of the main parameters of ASMaOEA, such as the threshold probability α for starting adaptive Pareto detection and the confidence p_e of the effective reference point. The following experiment uses fixed value patterns, and its test functions include the 5-, 8-, 10- and 15-objective MaF1, MaF2, MaF4 and MaF6 from CEC2017, where different values are set for the parameters analysed and the others use their default values.

4.3.1 Detection threshold probability α

The value of α determines the start time of the Pareto front detection operation. When the current iteration is $t > T * \alpha$,

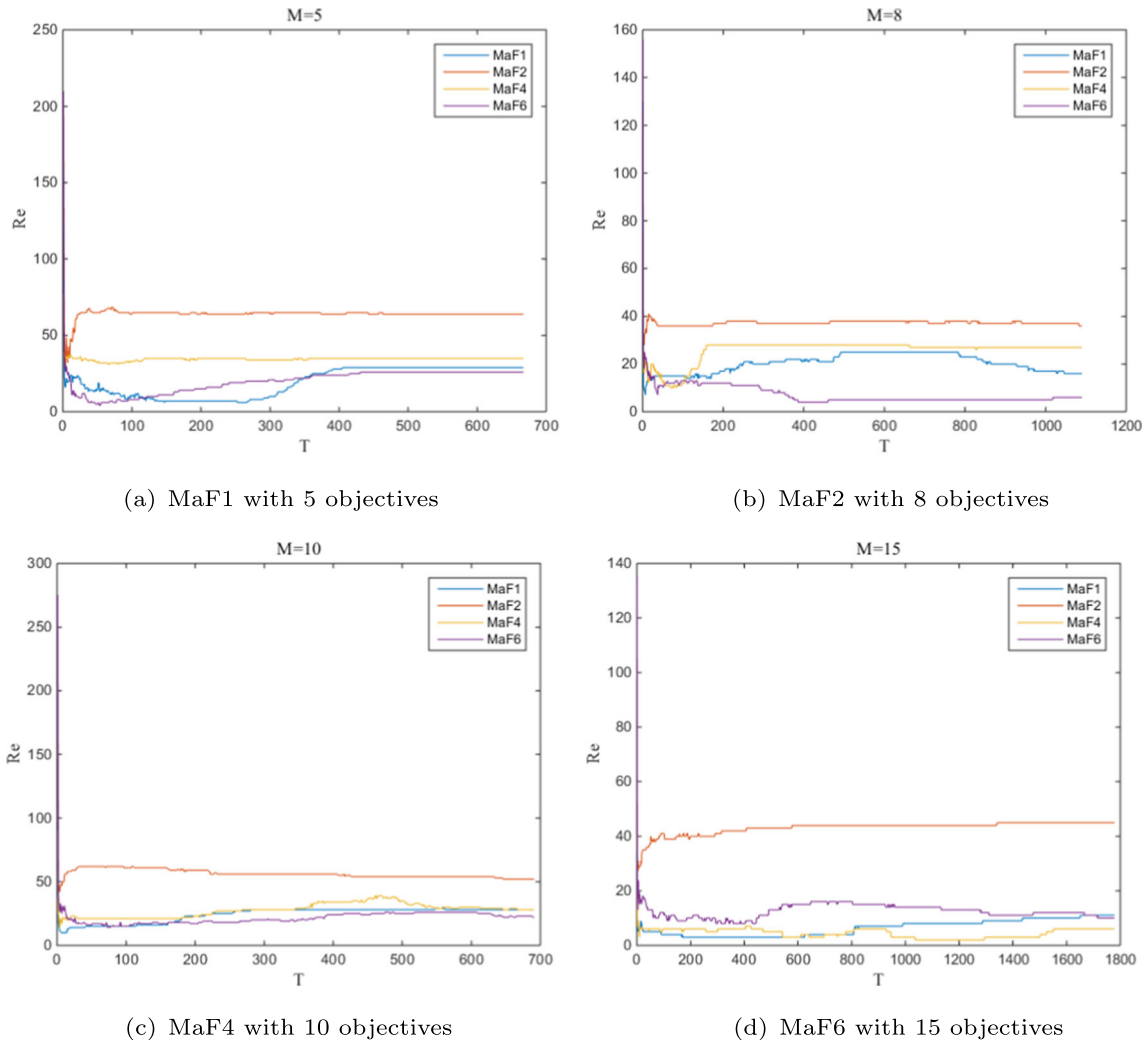


Fig. 3 Curve of the effective reference point R_e on MaF1, 2, 4, and 6

the algorithm starts to judge whether the Pareto front is degenerate or discrete. If the judgement is too early, the algorithm has not yet found all the valid reference points, so it will not fully utilize their leading function. On the other hand, because angle-based environment selection has high computational complexity, starting as late as possible helps save time overall. However, a late start can cause the optimization to fail to converge, hence degrading the overall performance.

This dilemma makes sensitivity experiments particularly important, as shown in Fig. 3a-d. Let us look at the specific results. The values on the Y-axis in Fig. 3 show that the effective reference points R_e change with the number of evolutions T on the X-axis for MaF1, 2, 4 and 6 with 5-, 8-, 10- and 15-objective problems, respectively. After $t > 400$ on the 5- and 10-objective problems, all significant reference points for MaF1, 2, 4 and 6 are found. On the 8-objective problem, the maximum effective reference point is obtained at $t > 500$ in Fig. 3b, and the best value is obtained after

$t > 800$ on the 15-objective problem in Fig. 3d. According to the above experiment on the 5-, 8-, 10-, and 15-objective test functions, $\alpha_{\min} = 400/700 \approx 0.57$, and it is recommended to take $\alpha = 0.6$ in the following simulation in Section 5.

4.3.2 Confidence of valid reference points p_e

Figure 4a-d show that the number of effective reference points R_e on the Y-axis changes with the iterative T value on the X-axis for the 8-objective problems for MaF1, 2, 4, and 6, respectively. When $p_e = 0.8$, the number of effective reference points is less than that of $p_e \in [0.3, 0.7]$. Typically, with a reasonable initial value in this scope, the algorithm will converge to the same or similar values of its valid reference points.

For example, on the 8-objective MaF1 and MaF6 problems, $p_e \in [0.3, 0.5]$ converges to the same value of 20 in Fig. 4a and d, while $p_e \in [0.6, 0.7]$ converges to 18. On the 8-objective MaF2, $p_e \in [0.3, 0.7]$ converges to a similar

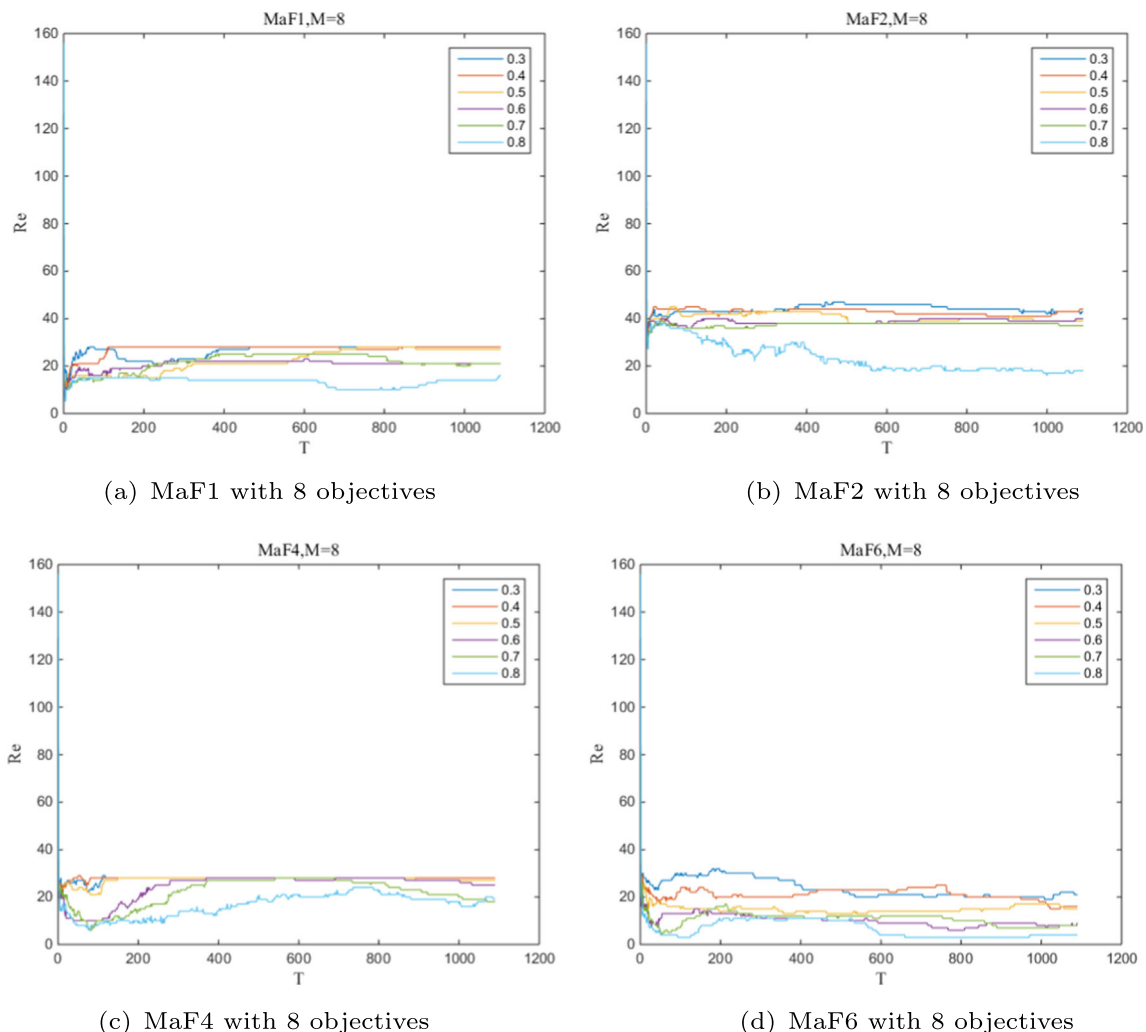


Fig. 4 Curve of R_e with T on MaF1, 2, 4, and 6

Table 2 Reference points and group sizes for problems with 5-15 objectives

$M-$	Reference points	Group size (N)
5	210	210
8	156	156
10	275	275
15	135	135

value of 40, as shown in Fig. 4b. On the 8-objective MaF4, $p_e \in [0.3, 0.6]$ converges to a similar value of 26, as shown in Fig. 4c. It is suggested that the range of p_e should be [0.4, 0.6], and 0.6 is its default value.

The confidence interval p_e affects the detection of an effective reference point for solving these complex problems. If the confidence level is set to a large value, the evaluation result will be smaller than the actual effective reference point; if the confidence level is too low, the effective reference point will be larger than the actual reference point. An accurate evaluation of p_e is beneficial for maintaining better diversity in ASMaOEA.

4.4 Time complexity of ASMaOEA

The time complexity of the ASMaOEA algorithm is mainly determined by adaptive partitioning pool selection, non-dominated sorting, the θ -dominated selection environment

Table 3 Mean and SD of HVs on MaF1-7 for ASMaOEA compared with MaOEA-CS, ANSGAIII, MOEA-D, RVEA* and RSEA

Prob.	M	ASMaOEA	MaOEA-CS	ANSGAIII	MOEA-D	RVEA*	RSEA	
MaF1	5	1.30E-02	1.31E-02	7.20E-03	1.12E-02	7.90E-03	1.11E-02	
		5.47E-04	4.71E-04	1.82E-03	<u>8.50E-05</u>	4.97E-04	4.48E-04	
		1.72E-05	1.22E-05	8.23E-06	<u>1.84E-07</u>	5.50E-06	9.57E-06	
	8	2.86E-05	2.74E-05	1.66E-05	4.26E-06	1.04E-05	2.20E-05	
		5.65E-07	1.58E-06	1.13E-07	<u>1.74E-08</u>	1.01E-07	1.94E-07	
		6.65E-07	5.00E-07	4.43E-07	2.02E-08	1.10E-07	4.72E-07	
	10	3.29E-01	0.00E+00	3.36E-12	9.11E-14	3.32E-13	2.85E-12	
		2.88E-02	0.00E+00	1.30E-12	<u>5.75E-16</u>	5.25E-13	1.88E-12	
		1.95E-02	1.21E-02	3.76E-02	<u>1.78E-03</u>	2.06E-02	1.09E-02	
	MaF2	5	1.98E-01	1.96E-01	1.85E-01	1.87E-01	1.90E-01	1.94E-01
			1.24E-02	5.99E-03	6.75E-03	<u>1.83E-03</u>	3.61E-03	5.28E-03
			2.17E-01	2.16E-01	2.13E-01	2.07E-01	1.91E-01	2.26E-01
8		2.02E-02	1.55E-02	4.40E-03	<u>1.24E-03</u>	2.88E-03	8.17E-03	
		2.24E-01	2.12E-01	2.26E-01	2.10E-01	1.86E-01	2.36E-01	
		1.68E-02	2.29E-02	1.47E-02	<u>1.11E-03</u>	9.85E-03	7.38E-03	
10		2.10E-01	2.09E-01	1.70E-01	1.78E-01	1.12E-01	4.89E-02	
		1.95E-02	1.21E-02	3.76E-02	<u>1.78E-03</u>	2.06E-02	1.09E-02	
		9.94E-01	9.99E-01	9.99E-01	9.89E-01	9.99E-01	8.97E-01	
MaF3		5	7.57E-03	1.52E-04	2.49E-03	4.73E-03	<u>2.26E-04</u>	4.75E-01
			9.88E-01	1.00E+00	9.59E-01	9.71E-01	1.00E+00	6.94E-01
			5.20E-03	<u>7.19E-06</u>	1.95E-01	5.69E-03	3.71E-05	8.58E-01
	8	5.46E-01	1.00E+00	3.59E-01	9.67E-01	1.00E+00	3.37E-01	
		1.79E+00	5.59E-06	1.42E+00	5.86E-03	<u>0.00E+00</u>	9.79E-01	
		9.35E-01	1.00E+00	9.79E-01	9.61E-01	1.00E+00	0.00E+00	
	10	4.61E-01	<u>2.54E-07</u>	5.02E-02	1.96E-03	9.07E-05	0.00E+00	
		1.21E-01	1.23E-01	7.33E-02	1.03E-02	1.18E-01	1.13E-01	
		7.94E-03	3.91E-03	3.50E-02	6.16E-03	1.08E-02	<u>3.75E-03</u>	
	8	2.53E-03	1.71E-03	2.30E-03	3.94E-06	4.46E-04	4.18E-03	
		2.18E-03	5.59E-04	6.67E-04	<u>3.57E-06</u>	3.46E-04	4.86E-04	
		2.85E-04	7.55E-05	2.51E-04	2.67E-08	5.84E-06	4.01E-04	
10	2.24E-04	3.74E-05	7.03E-05	<u>1.49E-08</u>	5.33E-06	3.89E-05		
	3.32E-08	0.00E+00	2.33E-07	2.62E-13	2.84E-11	3.05E-07		
	1.27E-07	0.00E+00	5.75E-08	<u>5.23E-14</u>	2.83E-11	9.02E-08		

Table 3 continued

Prob.	M	ASMaOEA	MaOEA-CS	ANSGAIII	MOEA-D	RVEA*	RSEA	
MaF5	5	8.13E-01	8.01E-01	8.12E-01	5.14E-01	7.78E-01	7.82E-01	
		<u>1.75E-03</u>	7.42E-03	1.37E-03	2.40E-01	1.22E-02	2.36E-02	
	8	9.24E-01	9.15E-01	8.98E-01	3.83E-01	8.26E-01	8.78E-01	
		<u>1.11E-03</u>	9.15E-03	2.13E-01	2.65E-01	6.86E-02	4.57E-02	
	10	9.70E-01	9.56E-01	9.69E-01	3.90E-01	9.65E-01	9.24E-01	
		<u>8.27E-04</u>	6.77E-03	1.72E-03	2.13E-01	6.83E-03	2.69E-02	
	15	9.91E-01	9.67E-01	9.86E-01	3.16E-01	9.63E-01	9.40E-01	
		<u>4.62E-04</u>	4.92E-03	3.43E-02	1.93E-01	2.07E-02	4.20E-02	
	MaF6	5	1.30E-01	1.30E-01	1.24E-01	1.13E-01	1.25E-01	1.24E-01
			1.30E-03	<u>1.08E-03</u>	7.47E-03	8.45E-02	3.66E-03	1.97E-02
8		1.06E-01	1.06E-01	9.63E-02	1.02E-01	1.03E-01	9.96E-02	
		1.06E-02	6.69E-04	2.94E-02	1.25E-02	<u>5.36E-04</u>	9.60E-03	
10		6.21E-02	1.01E-01	4.61E-02	9.99E-02	9.70E-02	9.29E-02	
		1.47E-01	<u>4.87E-04</u>	8.18E-02	1.90E-03	5.40E-03	2.65E-02	
15		9.54E-02	9.53E-02	8.99E-02	9.42E-02	9.30E-02	9.17E-02	
		1.18E-03	<u>6.63E-04</u>	2.39E-03	2.51E-03	1.99E-03	3.51E-03	
MaF7		5	2.62E-01	2.57E-01	2.52E-01	1.44E-01	2.74E-01	2.67E-01
			9.54E-03	1.10E-02	1.50E-02	<u>1.52E-03</u>	4.18E-03	1.65E-02
	8	2.03E-01	1.92E-01	2.00E-01	4.73E-05	1.93E-01	1.87E-01	
		1.84E-02	<u>8.73E-03</u>	1.90E-02	1.14E-05	2.34E-02	3.34E-02	
	10	1.97E-01	1.73E-01	1.75E-01	3.73E-04	1.58E-01	1.83E-01	
		2.33E-02	1.79E-02	2.28E-02	<u>3.48E-03</u>	1.53E-02	2.97E-02	
	15	1.63E-01	1.14E-01	1.30E-01	7.90E-06	8.38E-02	1.36E-01	
		3.32E-02	1.10E-02	3.30E-02	<u>3.37E-05</u>	3.48E-02	1.26E-02	

operation, and the angle-based selection strategy. For adaptive normalized partitioned pooling, the time complexity of the radial coordinate calculation is $O(MN)$, that of nondominated sequencing is $O[N(\log N)^{M-2}]$, and that of nondominated environment selection is $O(MN^2)$. The time complexity of angle selection is $O(N^2)$. In general, the time complexity of ASMaOEA is $O(MN^2)$.

5 Algorithm verification

In this section, we use several benchmarks, which are commonly used in sets of multiobjective problems, as well as the two most effective performance evaluation indices, inverted generational distance (IGD) and hypervolume (HV).

All experiments on ASMaOEA were conducted using MATLAB R2016b on the chosen problems. The operating system used was Windows 10, with 8 GB of RAM. The experimental results fully demonstrate that our algorithm performs very well.

5.1 Benchmark functions

This validation consists of 31 representative test functions, i.e., DTLZ1-7 [33], WFG1-9 [34], and MaF1-15 [35], where the latter were specified by the CEC 2017 international evolutionary algorithm open competition.

Two performance evaluation indices, IGD and HV [36], were used to reflect the convergence and diversity of the Pareto solutions. Better performance is indicated by a low IGD value or a high HV value [24].

Table 4 The versatility of various methods on MaF1-7

Method	Scope of Problems	Generalization ability
ASMaOEA	MaF1,2,5,6,7	5/7 = 71.429%
MaOEA-CS	MaF1,3,4,6	4/7 = 57.143%
ANSGAIII	MaF2	1/7 = 14.286%
MOEA-D	MaF1,2,4,7	0/7 = 0.000%
RVEA*	MaF3,7	2/7 = 28.571%
RSEA	MaF2,4	2/7 = 28.571%

Table 5 Mean and SD of HVs on MaF8-15 for ASMaOEA with MaOEA-CS, ANSGAIII, MOEA-D, RVEA* and RSEA

Prob.	M	ASMaOEA	MaOEA-CS	ANSGAIII	MOEA-D	RVEA*	RSEA
MaF8	5	1.26E-01	1.23E-01	1.09E-01	1.15E-01	9.32E-02	1.21E-01
		1.07E-03	<u>1.06E-03</u>	1.08E-02	4.78E-03	1.04E-02	9.43E-03
	8	3.07E-02	3.01E-02	2.39E-02	2.24E-02	7.51E-03	3.03E-02
		9.76E-04	<u>6.55E-04</u>	3.48E-03	1.21E-03	3.73E-03	9.57E-04
	10	1.11E-02	1.02E-02	8.92E-03	6.63E-03	3.95E-03	1.11E-02
		3.67E-04	2.63E-04	1.33E-03	3.81E-04	2.53E-03	<u>1.98E-04</u>
15	5.66E-04	5.75E-04	3.55E-04	1.87E-04	1.08E-04	5.82E-04	
	9.89E-05	<u>4.88E-05</u>	1.44E-04	7.78E-05	1.22E-04	7.01E-05	
MaF9	5	3.10E-01	2.93E-01	2.36E-01	3.12E-01	2.60E-01	2.24E-01
		1.27E-02	2.92E-02	1.61E-01	<u>7.93E-03</u>	9.31E-03	2.02E-01
	8	5.06E-02	4.97E-02	2.14E-02	4.14E-02	2.12E-02	4.61E-02
		<u>9.05E-04</u>	9.30E-04	3.26E-02	1.27E-03	4.44E-03	1.25E-02
	10	1.88E-02	1.70E-02	8.29E-03	1.44E-02	5.88E-03	1.71E-02
		<u>7.70E-04</u>	5.63E-04	2.76E-03	1.13E-03	8.35E-04	2.43E-03
15	1.17E-03	1.18E-03	4.48E-04	2.85E-04	1.80E-04	6.23E-04	
	1.42E-04	<u>1.19E-04</u>	8.02E-04	6.10E-04	1.09E-04	8.76E-04	
MaF10	5	9.93E-01	8.56E-01	9.42E-01	9.51E-01	8.44E-01	9.96E-01
		5.48E-03	2.89E-01	9.74E-02	4.83E-02	9.95E-02	<u>1.03E-03</u>
	8	9.99E-01	8.53E-01	9.99E-01	7.98E-01	9.14E-01	1.00E+00
		2.03E-03	8.75E-02	1.70E-03	2.08E-01	1.23E-01	<u>4.14E-04</u>
	10	9.97E-01	6.07E-01	9.99E-01	7.17E-01	8.79E-01	9.99E-01
		7.18E-03	1.85E-01	2.48E-03	3.00E-01	2.40E-01	<u>5.31E-04</u>
15	1.00E+00	1.00E+00	1.00E+00	5.01E-01	9.98E-01	1.00E+00	
	1.56E-04	2.92E-04	6.85E-04	4.79E-01	1.63E-04	<u>1.29E-04</u>	
MaF11	5	9.97E-01	9.93E-01	9.93E-01	9.64E-01	9.89E-01	9.95E-01
		<u>1.70E-03</u>	3.86E-03	2.24E-03	1.32E-02	1.89E-03	2.45E-03
	8	9.91E-01	9.97E-01	9.94E-01	9.40E-01	9.89E-01	9.98E-01
		7.71E-03	<u>2.07E-03</u>	8.83E-03	1.21E-02	4.72E-03	2.55E-03
	10	9.93E-01	9.98E-01	9.98E-01	9.37E-01	9.88E-01	9.98E-01
		5.73E-03	<u>1.31E-03</u>	4.23E-03	9.92E-03	5.97E-03	2.21E-03
15	9.92E-01	9.98E-01	9.93E-01	9.34E-01	9.92E-01	9.40E-01	
	3.17E-02	<u>1.90E-03</u>	1.02E-02	1.38E-02	4.40E-03	2.65E-01	
MaF12	5	7.73E-01	6.40E-01	7.40E-01	6.28E-01	7.25E-01	7.48E-01
		1.29E-02	2.14E-01	2.72E-02	1.65E-01	1.11E-02	<u>8.32E-03</u>
	8	8.38E-01	7.38E-01	7.41E-01	4.33E-01	8.02E-01	8.28E-01
		2.96E-01	1.87E-01	2.07E-01	2.34E-01	<u>1.24E-02</u>	1.65E-02
	10	9.05E-01	7.75E-01	8.59E-01	3.45E-01	8.30E-01	8.82E-01
		3.26E-02	1.83E-01	<u>2.01E-02</u>	3.37E-01	2.30E-02	2.39E-02
15	9.14E-01	7.66E-01	8.75E-01	1.95E-01	8.29E-01	8.76E-01	
	1.60E-01	2.29E-01	1.67E-01	4.28E-01	<u>7.45E-02</u>	8.87E-02	
MaF13	5	2.15E-01	2.60E-01	8.75E-01	2.65E-01	8.26E-02	2.14E-01
		9.70E-02	5.09E-02	1.67E-01	<u>2.11E-02</u>	1.32E-01	3.71E-02
	8	5.82E-02	1.38E-01	1.22E-01	9.29E-02	7.62E-02	9.82E-02
		9.58E-02	<u>2.10E-02</u>	5.86E-02	1.09E-01	7.55E-02	1.21E-01
10	3.08E-02	1.17E-01	1.11E-01	7.81E-02	8.11E-02	7.53E-02	

Table 5 continued

Prob.	M	ASMaOEA	MaOEA-CS	ANSGAIII	MOEA-D	RVEA*	RSEA
MaF14	15	1.53E-01	<u>1.63E-02</u>	4.36E-02	1.04E-01	1.57E-02	9.50E-02
		2.17E-02	7.24E-02	2.31E-02	3.16E-02	6.13E-02	9.92E-03
		9.75E-02	7.96E-02	8.96E-02	7.21E-02	<u>1.59E-02</u>	6.98E-02
	5	4.76E-01	6.02E-01	3.77E-01	1.93E-01	4.31E-01	2.73E-01
		2.60E-01	6.24E-01	3.52E-01	4.47E-01	<u>2.22E-01</u>	4.12E-01
		8	9.98E-02	3.46E-01	2.71E-02	8.53E-01	6.94E-01
	10	3.02E-01	4.77E-01	1.21E-01	<u>1.10E-01</u>	2.95E-01	1.61E-01
		1.51E-02	6.00E-01	5.15E-02	8.39E-01	7.13E-01	3.22E-03
		6.75E-02	4.75E-01	1.39E-01	4.46E-01	1.48E-01	<u>1.44E-02</u>
15	3.31E-01	7.02E-01	1.62E-02	1.43E-01	4.41E-01	1.85E-01	
	5.76E-01	3.59E-01	7.24E-02	2.32E-01	2.65E-01	<u>2.25E-01</u>	
	MaF15	5	9.02E-03	3.57E-02	9.56E-01	3.56E-02	2.16E-02
1.30E-02			2.82E-02	1.68E-01	3.62E-03	1.06E-02	<u>2.44E-04</u>
8			2.14E-04	1.41E-04	0.00E+00	1.83E-04	8.22E-05
10		5.86E-04	2.21E-04	0.00E+00	1.23E-04	4.87E-05	<u>2.67E-10</u>
		1.04E-05	5.62E-06	0.00E+00	5.31E-06	7.94E-07	0.00E+00
		2.03E-05	6.26E-06	0.00E+00	7.54E-06	<u>1.46E-06</u>	0.00E+00
15		9.38E-18	4.39E-11	1.15E-17	6.93E-11	3.48E-13	0.00E+00
		<u>3.12E-17</u>	1.16E-10	5.16E-17	1.03E-10	6.42E-13	0.00E+00

5.1.1 Inverted generational distance

The IGD is a comprehensive performance index. It can simultaneously evaluate the convergence, distribution, and uniformity of a solution set. It is defined as follows:

$$IGD(A, Z_{eff}) = \frac{1}{|Z_{eff}|} \sum_{i=1}^{|Z_{eff}|} \min_{j=1}^{|A|} \|(z_i - a_j)\|^2 \quad (13)$$

In (13), Z_{eff} is a set of evenly distributed target points on the real Pareto front. A is the final nondominated solution set obtained by the evaluated algorithm. The disadvantage of IGD is that we must know the real Pareto front of the optimization problem in advance.

5.1.2 Hypervolume indicator

Let S be a nondominated solution set, $S \in \Omega$; the reference point is denoted as $Ref = (r_1, r_2, \dots, r_m)$, where m is the dimension of its target space. The hypervolume index of the solution S is defined as the hypercube volume surrounded by the target space in which all the point sets in S and the reference point are located, expressed as $HV(S)$ in (14).

$$HV(S) = Leb(U_{X \in S} [f_1(X), r_1] \times \dots \times [f_m(X), r_m]) \quad (14)$$

where $Leb(S)$ represents the Lebesgue measure of the solution set S .

5.1.3 Choice of reference points

This section uses additional reference points. For any M -objective test function, 10000 reference points are uniformly sampled on the PF, and the final solution set is normalized to 1.1 times the nadir point of the PF; the HV is calculated by selecting the reference point $Ref = (r_1, r_2, \dots, r_m) = (1, 1, \dots, 1)$.

For the 5-, 8-, 10-, and 15-target problems, the group size is set as shown in Table 2, and the algorithm termination condition is the maximum evaluation function $FE_{max} = \max\{100000, 10000 * D\}$, where D defines the number of domain dimensions.

Table 6 Versatility of various methods on MaF8-15

Methods	Scope of Problems	Generalization Ability
ASMaOEA	MaF8,9,11,12,15	5/8 = 62.5%
MaOEA-CS	MaF9,11,13,14	4/8 = 50.0%
ANSGAIII	MaF13,15	2/8 = 25.0%
MOEA-D	MaF9,14,15	3/8 = 37.5%
RVEA*	MaF14	1/8 = 12.5%
RSEA	MaF8,10,11	3/8 = 37.5%

Table 7 Significance tests of six variants

		ASMaOEA	MaOEA-CS	ANSGAIII	MOEA-D	RVEA*	RSEA
ASMaOEA	B	—	28	36	44	40	36
vs.	E	—	17	17	9	9	11
	W	—	15	7	7	11	13

5.2 Comparative experiment and analysis

The performance of ASMaOEA is compared with that of 5 well-known algorithms (MaOEA-CS [37], ANSGAIII [24], MOEA-D [38], RVEA* [27] and RSEA [39]) on 7 test problems involving MaF1-7, and the average HV values are recorded in Table 3.

Due to the versatility of these various methods, we carefully analysed the data in Table 3. The 14 bold numbers in the third column of Table 3 are distributed among the five problems MaF1, 2, 5, 6, and 7, which means that ASMaOEA is sensitive to the validity of these problems. Therefore, its generalization ability is approximately equal to $5/7 = 71.429\%$. By comparison with the other algorithms, as shown in Table 4, we see that ASMaOEA outperforms them in terms of versatility.

Encouragingly, the greater the number of objectives is, the more reliable the performance of ASMaOEA. This may render it suitable for solving problems involving the high-dimensional uncertainty optimization of wireless cognitive networks. However, the stability and generalizability of ASMaOEA need to be further investigated experimentally on MaF3-4.

To fully understand the performance and characteristics of each algorithm, Table 5 lists the average HVs and standard deviations (SDs) of the MaF8-15 test functions on problems with 5-15 objectives for six relevant variants (ASMaOEA, MaOEA-CS, ANSGAIII, MOEA-D, RVEA* and RSEA).

The 11 bold numbers in the third column of Table 5 are distributed among five problems, which shows that ASMaOEA is valid in these five benchmark functions (MaF8,

9, 11, 12, and 15); that is, it is generalizable and robust in approximately $5/8 = 62.5\%$ of the cases. Table 6 lists the details about the versatility of the various algorithms on MaF8-15.

In Table 6, the MaOEA-CS and RSEA methods each achieve good performance on five benchmark functions (MaF8, 9, 11, 13, and 14 and MaF8, 10, 11, 14, and 15, respectively). As with MOEA-D on MaF9, MaF13 and MaF14, RVEA* has better effectiveness in solving MaF14; additionally, ANSGAIII performs well on MaF12 with 10 objectives, MaF13 with 5 objectives and MaF15 with 15 objectives.

Summarizing the performance of ASMaOEA on the MaF1-15 benchmark functions, combined with the characteristics of each benchmark function, we find that it has excellent performance in solving discrete, degraded and nonuniform problems (MaF5, MaF6, MaF8, MaF9, MaF11, MaF12, and MaF15), which verifies that the application of the Pareto frontier adaptive detection module of the algorithm is reliable. However, the performance of ASMaOEA in dealing with multipeak problems (MaF3, MaF4, and MaF14) is relatively weak, which is a direction that we can optimize in the future. Furthermore, although ASMaOEA does not exhibit the best stability on several benchmark functions, the standard deviation of HV significantly decreases as the dimensionality of the problem increases. For instance, on MaF15, as the objective dimensionality increases from 5 to 15, the SD decreases from $1.30E-02$ to $3.12E-17$, reaching the optimal value. These findings demonstrate the potential of our algorithm for addressing high-dimensional problems.

Fig. 5 The average inverted generational distance (IGD) for different objectives with different algorithms

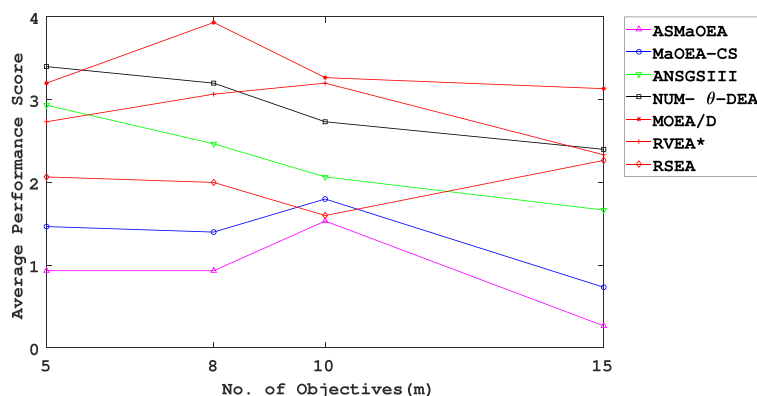
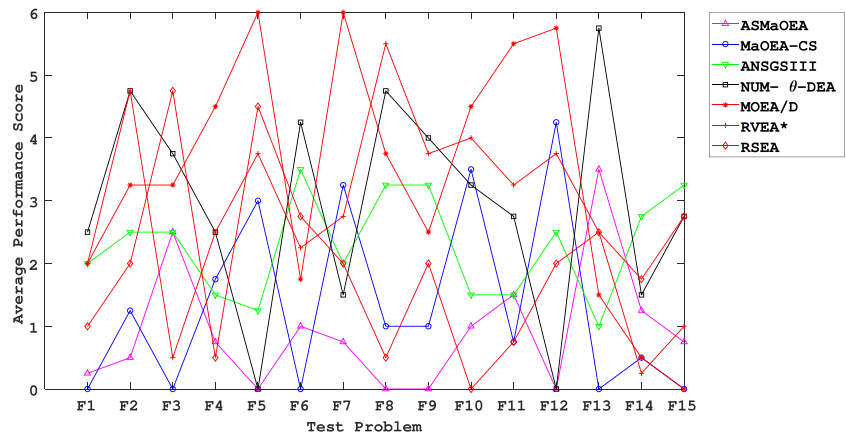


Fig. 6 The average inverted generational distance (IGD) values on MaF1-15 for different algorithms



5.3 Statistical Significance Tests

This subsection describes the statistical significance of the data of the 15 multiobjective optimization functions MaF1-15 for each of the 4 categories (5-, 8-, 10- and 15-objective) in a total of 60 independent comparison experiments. A Wilcoxon rank sum test with significance value 0.05 was performed for each pair of algorithms.

Table 7 shows the results of the significance test of ASMaOEA compared with other variants. “B” (“W”) indicates that Algorithm 1 is significantly superior (inferior) to Algorithm 2, and “E” indicates that there is no statistically significant difference between Algorithm 1 and Algorithm 2.

In Table 7, taking the fourth column of MaOEA-CS as an example, in 60 experiments comparing it with MaOEA-CS, ASMaOEA won 28 rounds, tied in 17 rounds, lost 15 rounds, and achieved 13 wins in terms of performance. The fifth column shows that ASMaOEA won 36 rounds, tied 17 rounds, and lost seven rounds against ANSGAIII.

5.4 Average Score of IGD

To show the overall performance of each algorithm, the average value of the IGD was used to rank them.

Figure 5 shows the average inverted generational distance in the 5-, 8-, 10- and 15-objective problems for the ASMaOEA, MaOEA-CS, ANSGAIII, NUM-θ-DEA, MOEA-D, RVEA* and RSEA algorithms. The average IGD of ASMaOEA on the problems with 5-15 objectives is the smallest, indicating that it is robust against these problems.

Table 8 The three kinds of preference scenarios

Object	Weights of scenarios		
	Emergency	High-speed	Low-power
f_{be}	0.8	0.1	0.1
f_p	0.1	0.1	0.8
$f_{thr.}$	0.1	0.8	0.1

Its IGD had a prominent value of less than 0.5 for 15 objectives, and it maintained a value no greater than one in all cases, except for 10-objective problems. Figure 6 shows the average values of the seven algorithms in terms of the IGD of the test function (MaF1-15) and underscores the impressive performance of ASMaOEA in most cases.

According to the HV and IGD values, no single method was absolutely superior. Comparison is a detailed task and involves many factors. However, according to the significance test and performance score, the above experimental results show that the proposed ASMaOEA has a significant advantage over the other methods tested in that it avoids the degradation of reference points and solves high-dimensional problems.

6 Simulation and application

This section explores the effects of ASMaOEA and its parameters proposed in the previous section and compares its

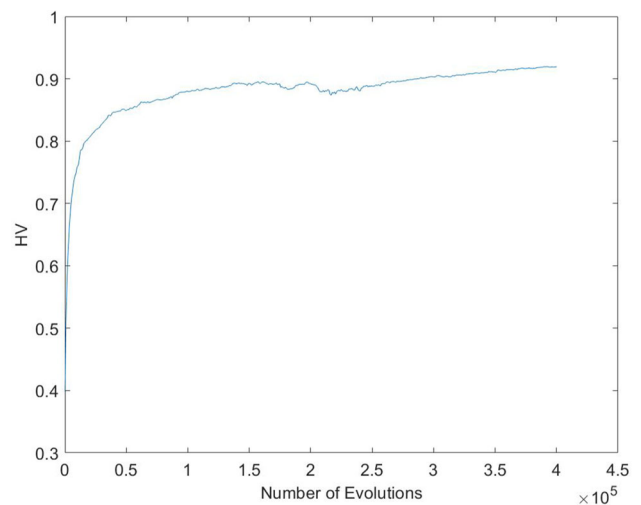


Fig. 7 The mean HV varying during the evaluations

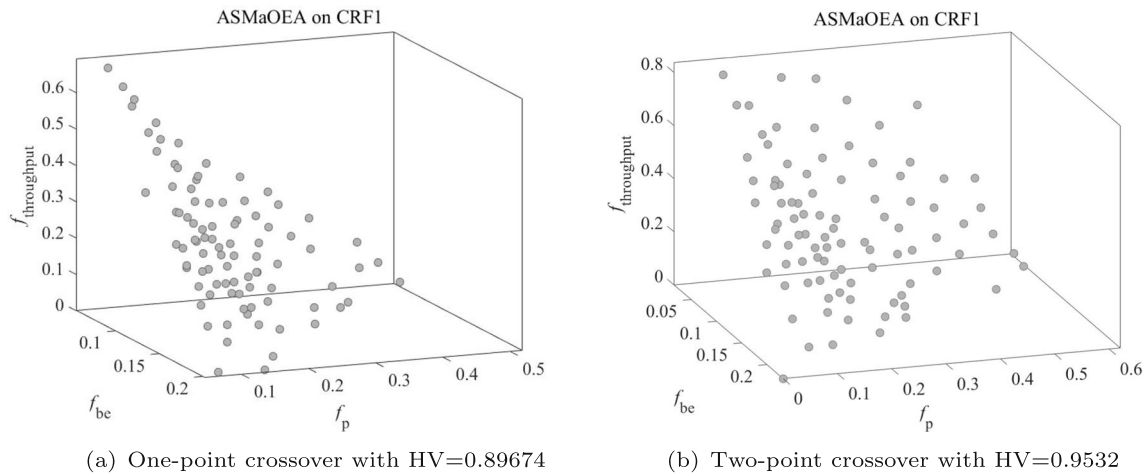


Fig. 8 Distribution of ASMaOEA solutions on CRF1

performance with those of MaOEA-CS, ANSGAIII, NUM- θ -DEA, MOEA-D, RVEA* and RSEA in problem CRF1 for the Pareto front distribution without any preference.

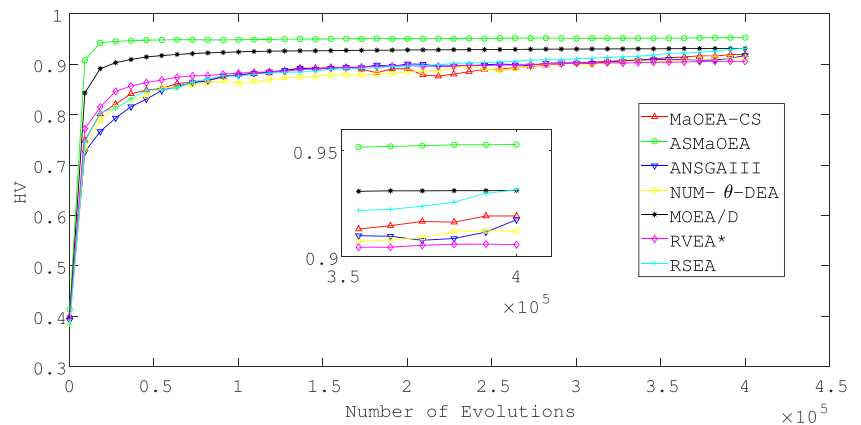
There are three typical preference scenarios for cognitive radio decision engine simulations that require real-time parameter optimization: 1) an emergency scenario requiring high reliability, 2) a low-power scenario with an energy-saving mode, and 3) a high-throughput scenario requiring a high-efficiency mode. In this section, we first apply ASMaOEA to the CRF1 problem and then choose the solutions from the Pareto fronts based on the scenarios.

Table 8 shows the weights corresponding to the three preferred scenarios in a running stage and gives the configuration of the relevant parameters.

6.1 Initialization

Figure 7 shows that the HV of ASMaOEA changes with the number of evaluations. When $k = 5$, the HV tends to converge and reach a maximum; therefore, the condition $k = 5$ is reasonable, and the reference point of HV $r = [1 \ 1 \ 1]$.

Fig. 9 Variation in HV with respect to CRF1 for each algorithm



In the Gaussian white noise channel, the transmit power ranges from 0 to 25.2 dBm, and its interval is set to 0.4 dBm. The modulation scheme can use any of four types (BPSK, QPSK, 16QAM or 64QAM) and maintain the symbol rate $R_s = 1$ Mbps. The optimization of formula CRF1 is a 3-objective problem, so the population size N is set to 91. The termination condition is the maximum evaluation $FE_{max} = 10000 * k * c_l$, where c_l is the code length of the subcarrier, $K \in \{1, 2, 3, 4, 5\}$.

Because the decision-making domain is a binary code, the bitwise mutation may determine whether one or two points are used as the crossover operator; Fig. 8a and b show the distributions of the Pareto front solutions and their HVs, respectively. We can see that the two-point crossover operator is more suitable than the one-point crossover operator. When the mutation probability is $p_m = 1/D$, $D = 256$ represents the individual encoding length.

6.2 Cognitive Decision Engine Optimization

The Pareto solution set of the CRF1 problem was solved by ASMaOEA and compared with the results of MaOEA-CS,

Table 9 Comparison of the mean HV and standard deviation on CRM1 obtained by the seven algorithms

Algorithm	HV Mean	HV Standard Deviation
MaOEA-CS	9.193E-01	1.536E-02
ASMaOEA	9.530E-01	1.977E-03
ANSGAIII	9.176E-01	2.861E-02
NUM- θ -DEA	9.121E-01	9.590E-03
MOEA-D	9.314E-01	3.895E-03
RVEA*	9.058E-01	8.390E-03
RSEA	9.317E-01	1.067E-02

The bold numbers are the optimal values for their respective columns

ANSGAIII, NUM- θ -DEA, MOEA-D, RVEA* and RSEA. Since the Pareto front of the problem to be optimized is unknown, only HV values can be used to evaluate the convergence and diversity of the Pareto solutions, as shown in Fig. 9.

Figure 9 shows the change in the HV of ASMaOEA and the other algorithms with the number of evaluations, where the ASMaOEA HV converges most rapidly at the beginning and remains basically unchanged at the later stage. The HV of the MaOEA-CS algorithm varies with the number of evaluations. After 15,000 iterations, ASMaOEA always maintains its leading edge. Notably, its HV remains above 0.95. The other 5 variants also achieved good scores, above 0.90, after 15,000 iterations.

Table 9 shows the HV mean and standard deviation on CRM1 obtained by ASMaOEA and the other six algorithms. In terms of the mean HV (9.530E-01) and standard deviation (1.977E-03), ASMaOEA achieved the best performance on the CRF1 problem, while the performance of MaOEA-CS was in the middle.

Figures 8b and 10a-f show the distribution of the Pareto fronts of ASMaOEA, MaOEA-CS, ANSGAIII, NUM- θ -DEA, MOEA-D, RSEA and RVEA* on CRF1 and their HV values, respectively. The Pareto fronts obtained by ASMaOEA and RSEA on CRF1 are very strong in searching the target area, and they can reach approximately 0.8 for $f_{throughput}$, which is a promising value. MOEA-D is characterized by a very even distribution of solutions, while the diversity and convergence of the NUM- θ -DEA and ANSGAIII solutions are at the same level.

6.3 Comparisons of several algorithms on CRF1

As shown in Table 10, for the high-speed scenarios, both ASMaOEA and MOEA-D yielded a minimum power of 0.4 dBm, and the average power of MaOEA-CS was 0.52 dBm while guaranteeing a maximum throughput of 6 Mbps; all the algorithms chose 64QAM as the encoding method.

Table 10 shows the distribution of the data rate (Mbps/s), transmission power, and BER in each channel obtained via ASMaOEA in three CRF1 scenarios. The overall BER of the

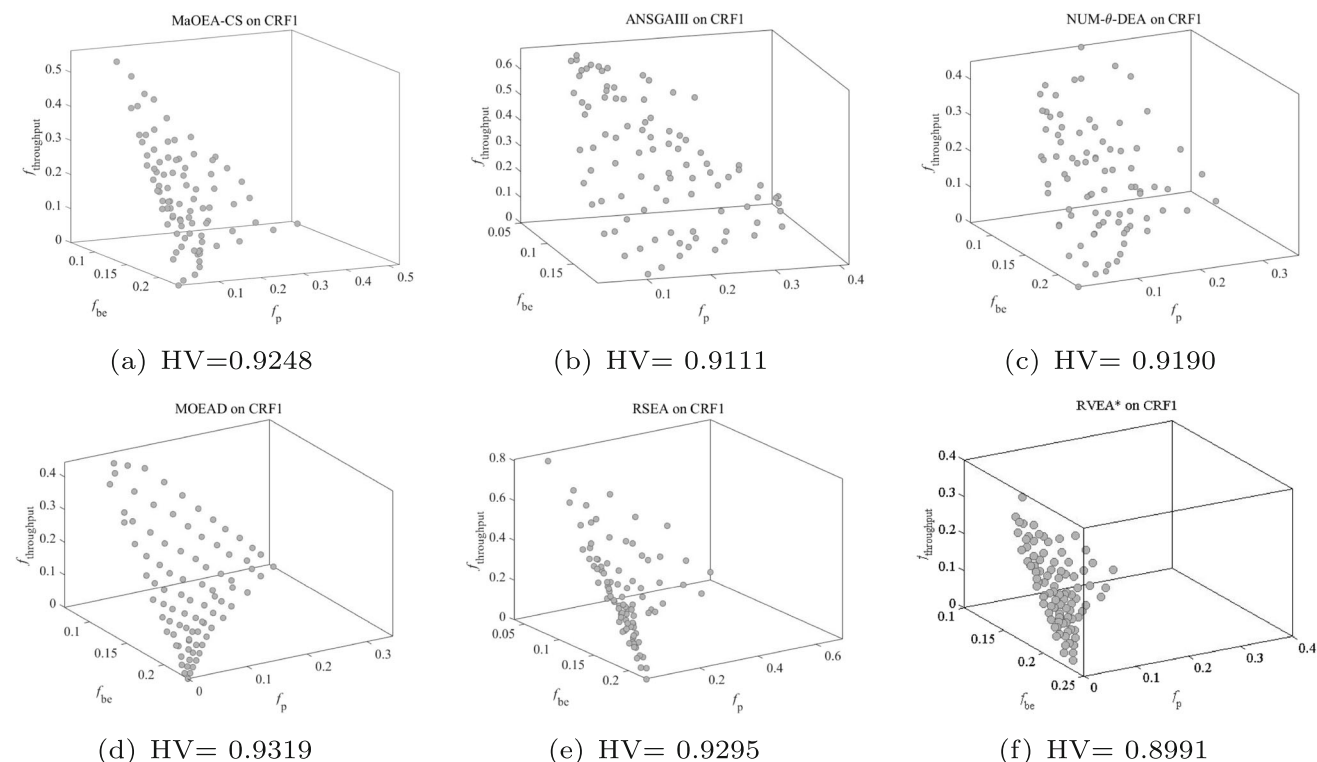
**Fig. 10** Pareto fronts of MaOEA-CS, ANSGAIII, NUM- θ -DEA, MOEA-D, RSEA and RVEA* on CRF1 and their HVs

Table 10 The mean of f_{be} , f_p^* (dBm), and f_{thr} (Mbps) for MaOEA-CS, ASMaOEA, ANSGAIII, NUM θ -DEA, MOEA-D, RVEA* and RSEA in three typical CRF1 scenarios

Algorithm	Obj./Scenario	Emergency	High-speed	Low-power
MaOEA-CS	f_{be}	7.96E-06	4.59E-02	4.59E-02
	f_p	11	0.52	0.52
	f_{thr}	5.59	6.00	6.00
ASMaOEA	f_{be}	1.10E-14	4.68E-02	4.68E-02
	f_p	15.79	0.4	0.4
	f_{thr}	5.98	6.00	6.00
ANSGAIII	f_{be}	3.95E-06	1.54E-02	2.58E-02
	f_p	10.04	3.94	1.26
	f_{thr}	5.53	6.00	5.06
NUM- θ -DEA	f_{be}	1.70E-04	4.58E-02	4.58E-02
	f_p	6.70	0.51	0.51
	f_{thr}	5.19	6.00	6.00
MOEA-D	f_{be}	2.07E-05	4.68E-02	4.68E-02
	f_p	8.53	0.4	0.4
	f_{thr}	5.82	6.00	6.00
RVEA*	f_{be}	1.00E-03	3.97E-02	3.54E-02
	f_p	6.37	0.99	0.46
	f_{thr}	5.69	6.00	5.69
RSEA	f_{be}	1.95E-09	4.31E-02	4.31E-02
	f_p	17.57	0.79	0.793
	f_{thr}	5.81	6.00	6.00

The bold numbers are the optimal values for their respective columns

channel was 0.01. In general, ASMaOEA had the best strategies for the three scenarios, and its average BER remained under 0.0001. Faced with complex requirements, its optimization results can ensure a lower error rate and promising system throughput.

7 Conclusion

The cognitive engine has a very large decision-making space. The goals of the minimum bit error rate, minimum power, and maximum system throughput conflict, yielding a multiobjective optimization problem. This study explored a strategy to estimate the eigenvalues of the Pareto front efficiently so that θ -DEA can be applied to uniform, degenerate, and discrete Pareto fronts simultaneously. After studying the parental selection and environment selection mechanisms in prevalent multiobjective algorithms, we propose an algorithm called ASMaOEA. ASMaOEA is effective according to the results of a significance test and other performance evaluations. However, ASMaOEA exhibits suboptimal performance in terms of stability, particularly when the number of objectives is low. We will focus on enhancing its stability in future work. Moreover, in the application of cognitive radio resource allocation, we consider only three dimensions of the objectives. More variables will be used in our future

work, such as the coding rate, packet length, time-division duplexing, bandwidth, and other factors of decision making. In the target domain, we plan to further minimize interference and maximize spectral efficiency to render the model suitable for higher-dimensionality problems.

Acknowledgements This work is partly supported by the National Natural Science Foundation of China (No. 61572074) and the Key Technologies Research and Development Program of China (No. 2020YFB1712104).

Funding This work is partly supported by the National Natural Science Foundation of China (No. 61572074) and the Key Technologies Research and Development Program of China (No. 2020YFB1712104).

Data Availability Data sharing was not applicable to this article, as no datasets were generated or analysed during the current study.

Code Availability The code used in the study is available from the corresponding author upon reasonable request.

Declarations

Conflicts of interest Author Hong-Bo Wang declares that he has no conflicts of interest. Author Yi-Zhe Wang declares that she has no conflicts of interest. Author Fan-Bing Zeng declares that she has no conflicts of interest. Author Jin Wang declares that he has no conflicts of interest.

Ethical approval This article does not contain any studies with human participants or animals performed by any of the authors.

Open Access This article is licensed under a Creative Commons Attribution 4.0 International License, which permits use, sharing, adaptation, distribution and reproduction in any medium or format, as long as you give appropriate credit to the original author(s) and the source, provide a link to the Creative Commons licence, and indicate if changes were made. The images or other third party material in this article are included in the article's Creative Commons licence, unless indicated otherwise in a credit line to the material. If material is not included in the article's Creative Commons licence and your intended use is not permitted by statutory regulation or exceeds the permitted use, you will need to obtain permission directly from the copyright holder. To view a copy of this licence, visit <http://creativecommons.org/licenses/by/4.0/>.

References

- Ilyas M, Ucan ON, Bayat O, Yang X, Abbasi QH (2018) Mathematical modeling of ultra wideband in vivo radio channel. *IEEE Access* 6:20 848–20 854
- Hoang TD, Le LB (2017) Joint prioritized scheduling and resource allocation for OFDMA-based wireless networks. *IEEE Trans Wirel Commun* 17(1):310–323
- Yang C, Li J, Guizani M, Anpalagan A, ElKashlan M (2016) Advanced spectrum sharing in 5G cognitive heterogeneous networks. *IEEE Wirel Commun* 23(2):94–101
- Yuan Y, Xu H, Wang B, Yao X (2015) A new dominance relation-based evolutionary algorithm for many-objective optimization. *IEEE Trans Evol Comput* 20(1):16–37
- He A, Gaedert J, Bae KK, Newman TR, Reed JH, Morales L, Park CH (2009) Development of a case-based reasoning cognitive engine for IEEE 802.22 WRAN applications. *ACM SIGMOBILE Mobile Comput Commun Rev* 13(2):37–48
- Park JH, Lee WC, Choi JP, Choi JW, Um SB (2018) Applying case-based reasoning to tactical cognitive sensor networks for dynamic frequency allocation. *Sensors* 18:4294
- Huang Y, Jiang H, Hu H, Yao Y (2009) Design of Learning Engine Based on Support Vector Machine in Cognitive Radio. In: 2009 International conference on computational intelligence and software engineering, pp 1–4
- Eisen M, Ribeiro A (2020) Optimal Wireless Resource Allocation With Random Edge Graph Neural Networks. *IEEE Trans Signal Process* 68:2977–91
- Meng F, Chen P, Wu L, Cheng J (2020) Power Allocation in Multi-User Cellular Networks: Deep Reinforcement Learning Approaches. *IEEE Trans Wirel Commun* 19(10):6255–67
- Rondeau TW, Le B, Maldonado D, Scaperth D, Bostian CW (2006) Cognitive Radio Formulation and Implementation. In: 2006 1st International conference on cognitive radio oriented wireless networks and communications, pp 1–10
- Alqerm I, Shihada B (2014) Adaptive Decision-Making Scheme for Cognitive Radio Networks. 2014 IEEE 28th International Conference on Advanced Information Networking and Applications. Victoria, BC, Canada, pp 321–328
- Zhao ZJ, Hai-chao L, editors (2012) A cognitive engine based on case-based reasoning quantum genetic algorithm. In: 2012 IEEE 14th international conference on communication technology, pp 224–228
- Alqerm I, Shihada B (2017) Energy-Efficient Power Allocation in Multitier 5G Networks Using Enhanced Online Learning. *IEEE Trans Veh Technol* 66(12):11086–97
- Zhao N, Li S, Wu Z (2012) Cognitive Radio Engine Design Based on Ant Colony Optimization. *Wirel Pers Commun* 65(1):15–24
- Zhao Z, Xu S, Zheng S, Shang J (2009) Cognitive radio adaptation using particle swarm optimization. *Wirel Commun Mobile Comput* 9(7):875–881
- Nebro AJ, Durillo JJ, Machín M, Coello Coello CA, Dorronsoro B (2013) A Study of the Combination of Variation Operators in the NSGA-II Algorithm. In: Advances in artificial intelligence, pp 269–278
- Tan X, Zhang H, Hu J (2014) A hybrid architecture of cognitive decision engine based on particle swarm optimization algorithms and case database. *Annals of telecommunications-Annales des télécommunications* 69(11–12):593–605
- Aryal SR, Dhungana H, Paudyal K (2012) Novel approach for Interference Management in cognitive radio. In: 2012 Third Asian Himalayas International Conference on Internet, pp 1–5
- Zhu Q, Tang H, Huang J, Hou Y (2021) Task scheduling for multi-cloud computing subject to security and reliability constraints. *J IEEE/CAA Automatica Sinica* 8(4):848–865
- Yadav SK, Kumar R (2023) EVACON-Rainbow Computing: An Amalgamation of Cloud and Its Inherited Computing to Encourage End User for Both Localized and Globalized Remote Computing. *Wireless Pers Commun* 132: 2737–2792 <https://doi.org/10.1007/s11277-023-10741-5>
- Liu L, Wang N, Chen Z, Guo L (2018) A Novel Spectrum Scheduling Scheme with Ant Colony Optimization Algorithm. *Algorithms [Internet]* 11(2):16
- El-Malek AHA, Aboulhassan MA, Abdou MA (2020) Evolutionary computation technique enhancing the performance of cognitive radio networks with energy harvesting. *Ad Hoc Netw* 107:102254
- Abbasi H, Yaghoobi M (2023) Optimized cascade chaotic fuzzy system (OCCFS) and its application to function approximation and chaotic systems identification. *Soft Comput* 27: 8561–8582 <https://doi.org/10.1007/s00500-023-08171-3>
- Deb K, Jain H (2013) An evolutionary many-objective optimization algorithm using reference-point-based nondominated sorting approach, part I: solving problems with box constraints. *IEEE Trans Evol Comput* 18(4):577–601
- Li M, Yang S, Liu X (2014) Shift-Based Density Estimation for Pareto-Based Algorithms in Many-Objective Optimization. *IEEE Trans Evol Comput* 18(3):348–65
- Venkatraman S, Yen GG (2005) A generic framework for constrained optimization using genetic algorithms. *IEEE Trans Evol Comput* 9(4):424–35
- Cheng R, Jin Y, Olhofer M, Sendhoff B (2016) A Reference Vector Guided Evolutionary Algorithm for Many-Objective Optimization. *IEEE Trans Evol Comput* 20(5):773–91
- Zhang X, Tian Y, Cheng R, Jin Y (2018) A Decision Variable Clustering-Based Evolutionary Algorithm for Large-Scale Many-Objective Optimization. *IEEE Trans Evol Comput* 22(1):97–112
- Jiang S, Yang S (2017) A strength Pareto evolutionary algorithm based on reference direction for multi-objective and many-objective optimization. *IEEE Trans Evol Comput* 21(3):329–346
- Li MQ, Yao X (2020) What Weights Work for You? Adapting Weights for Any Pareto Front Shape in Decomposition-Based Evolutionary Multiobjective Optimisation. *Evol Comput* 28(2):227–253
- Zhao Z-J, Zheng S-L, Shang J-N, Kong X-Z (2007) A study of cognitive radio decision engine based on quantum genetic algorithm. *Acta Physica Sinica* 56(11):6760–6
- Patil VM, Patil SR (2016) A survey on spectrum sensing algorithms for cognitive radio. In: 2016 International conference on advances in human machine interaction (HMI)
- Deb K, Thiele L, Laumanns M, Zitzler E (2005) Scalable Test Problems for Evolutionary Multiobjective Optimization. *Theoretical Advances and Applications, London, Evolutionary Multiobjective Optimization*

34. Huband S, Barone L, While L, Hingston P, editors. A Scalable Multi-objective Test Problem Toolkit. In: Proceedings of the third international conference on evolutionary multi-criterion optimization (EMO'05), Springer-Verlag, Berlin, Heidelberg, pp 280–295
35. Cheng R, Li M, Tian Y, Zhang X, Yang S, Jin Y, Yao X (2017) A benchmark test suite for evolutionary many-objective optimization. *Complex Intell Syst* 3(1):67–81
36. Yen GG, He Z (2014) Performance Metric Ensemble for Multiobjective Evolutionary Algorithms. *IEEE Trans Evol Comput* 18(1):131–44
37. Sun H, Cai X, Sulaman M, Fan Z (2017) An Evolutionary Many-Objective Optimization Algorithm Based on Coverage and Cache Strategy. 2017 International Conference on Industrial Informatics - Computing Technology, Intelligent Technology, Industrial Information Integration (ICIICII), pp 108–111
38. Zhang Q, Li H (2007) MOEA/D: A Multiobjective Evolutionary Algorithm Based on Decomposition. *IEEE Trans Evol Comput* 11(6):712–31
39. He C, Tian Y, Jin Y, Zhang X, Pan L (2017) A radial space division based evolutionary algorithm for many-objective optimization. *Appl Soft Comput* 61:603–21

Publisher's Note Springer Nature remains neutral with regard to jurisdictional claims in published maps and institutional affiliations.